Strain-Energy Criterion based Method of Numerical Simulation for Trabecular Bone Remodeling — (Ⅱ) Proximal Femur Remodeling*

Bingzhi Chen, Yuanxian Gu, Zhan Kang, Shutian Liu
State Key Laboratory of Structural Analysis for Industrial Equipment,
Dept. of Engineering Mechanics, Dalian University of Technology, Dalian 116024, China

Abstract. Combined with the finite element method, an optimization algorithm based on strain-energy density criterion is proposed in this paper for the numerical simulation of the internal remodeling of trabecular bones. The strain-energy density is taken as the mechanical stimulus, and the bone remodeling is described with the change of material density distribution, which can represent the internal remodeling of trabecular bones. The numerical results of the remodeling simulation for proximal femur both in three- and two-dimensional models have been presented. It is demonstrated that (1) this method produced a realistic apparent density distribution in the proximal femur. (2) The numerical results of presented in the paper are in accordance with the practical phenomena.

Keywords: bone remodeling; bone adaptation; strain-energy density; resorption; formation; Femur;

1. Introduction

The stress and growth is the key problem in the study of biomechanics. More than 100 years ago, Culmann and von Meyer noted a qualitative likeness between the trabecular architecture in the femur and principal stress trajectories in a similarly shaped crane. In 1892, Wolff put forward his “law of bone transformation”, that the trabecular of cancellous bone align with the directions of principal stress and when the loading environment changes, the trabecular reorient along the new stress trajectories. From the Wolff’s, the research was developed alone these two ways. The one is so called adaptive elasticity theory, which use some average strain, strain energy or stress measure as the remodeling stimulus. If the strain, strain energy or stress exceeds the value of equilibrium state, the bone will be remodeled. There always exists one equilibrium state in the bone. The other one is so called bone maintenance theory, which was developed by Carter and colleagues. This theory uses an average measure of the entire stress history for the remodeling stimulus. Variations of bone maintenance theory have been used to study bone development, adaptation and fracture healing.

The theory of adaptive elasticity presented by Cowin and Hegedus (1976), was the first mathematically rigorous theory for adaptive growth and remodeling of bones. The theory of adaptive elasticity regarded the average strain energy as the main stimulus to explain the bone remodeling phenomena. In another study, Firoozbakhsh and Cowin (1980) investigated the remodeling behavior of an initially inhomogeneous, orthotropic cylinder subjected to a period axial compressive load. The other famous rule about bone remodeling is “maximum-minimum principle”, which was adopted by Roux (1881) first. The maximum-minimum principle means that a maximum strength of bone is achieved with a minimum of constructional material. Curry (1984), Subbarayan and Bartel (1989) have incorporated the maximum-minimum approach and, in particular, Fyhrie and Carter (1986) used such an approach to make qualitative predictions of density and trabecular alignment. More recent studies on adult animals in vivo (Chow et al., 1993) have shown a dose-response relationship between the applied loads and the formation rate of trabecular bones, and suggested that the shape and thickness of individual trabecular are modeled by loads. Fyhrie and Schaffler (1995) used the method of strain tolerate error which led to trabecular remodeling, studying the relationship between strain and apparent density of trabecular. Charels et al (1997) and Christopher et al (1997) discussed the relationship between density distribution and modeling stimulus. Bone maintenance theory has also been developed these years. Stipner (1995), Huiskes (1992) and Poss et al (1988) considered the two-dimensional model of femur and studied the remodeling phenomenon of stress accumulate.

In this paper, on the basis of the structural optimization theory and the finite element analysis method, one numerical simulation method to predict bone remodeling is proposed. Utilizing the adaptive elasticity theory of bone remodeling and taking element material density as design variable, the internal modeling of trabecular bones can be formulated as an inverse problem of material distribution. An optimization algorithm based on the strain energy density criterion is proposed to solve the inverse problem the internal remodeling of trabecular bones. The strain energy density is taken as the mechanical stimulus, and the bone internal remodeling is described with the distribution of material density, which is the optimization variable. In the meanwhile,

* The project supported by the Scientific Fund for National Outstanding Youth of China (19525206) and the NKBRSF of China (No. G1999032805).

combined by the clinic situation, the time dependency of bore remodeling and the simulation of dead zone are considered here. The computation is implemented in the software JIFEX developed for the structural finite element analysis and design optimization. As examples, the two-dimensional and three-dimensional models of femur proximal end are calculated. It is shown that the numerical simulation provides results which are in accordance with the actual situation, and which reflect the time dependency of bone remodeling and the influence of dead zone effects.

2. Numerical Simulation Method

On the basis of the adaptive elasticity theory (proposed by Cowin et al.1976) and strain energy criterion (proposed by Charles et al.1997), non-linear factors are introduced, the dead zone considered, and bone optimization equations are proposed. It is combined with bone optimization equations and finite element method to solve the problem of bone remodeling. The true two or three-dimensional femur proximal model is taken as our research objective, and then, through simulation, the inner material distribution of femur proximal end is computed.

2.1 Governing equation of the strain-energy criterion

The strain energy within the bone, denoted as U, can be expressed by the stresses and strains as

$$U = \frac{1}{2}\{\sigma\}\{\varepsilon\} \tag{1}$$

From these mechanical variables, a stimulus is determined, which controls the rate of bone remodeling. The relation between the strain energy stimulus and the rate of change of bone density can be described in a remodeling governing rule. The actual bone density is then related to the modulus of elasticity of the bone, hence an updated input for the FEM model. The objective used in the simulation is total strain energy, which has already described in equation (1). The iterative procedure stops when the objective is reached or when the bone density has reached its maximum or minimal value. So the remodeling governing equation is stated as:

$$\frac{1}{n}\sum_{i=1}^{n}\frac{U_i}{\rho} = \frac{U_a}{\rho} \tag{2}$$

$$\Delta\rho = B\left(\frac{U_a}{\rho} - k\right) \tag{3}$$

where U_i (MPa) is the strain energy density (SED) for loading case i, as calculated in a continuum model of the bone material. Ua is the average SED over all n loading cases, ρ (g/cm^3) is the apparent density and $\Delta\rho$ is a change of density, k is a constant called reference stimulus, B is the remodeling coefficient, which is time dependent. Eq.(3) is the bone remodeling governing equation of the strain-energy criterion.

The value of k is fixed in the specific period and human. The quantity Ua/ρ (Joules/gram) represents the remodeling stimulus and is assumed to be sensed by bone specimen cells. It depends on the quantity Ua/ρ to determine whether bone formulation or resorption is taken for the case that place. When Ua/ρ-k≠0, there is a driving force which led to bone formation or resorption. When the driving force is negative, bone resorption occurs, while the driving force is positive, the force will induce bone formation. However, that is not so simple in practice. When driving force Ua/ρ exceed or lower than the reference stimulus k in a less range, the bone remodeling will not occur, which is called dead zone. Bone remodeling will not be induced if there exists a small difference between the actual strain energy density and reference strain-energy density k. Hence, there always exists one specific dead zone s. Eq.(3) can be described as following

$$\frac{d\rho}{dt} = B\left\{\frac{U_a}{\rho} - k(1+s)\right\}, \quad \text{if } U_a/\rho \geq k(1+s), \tag{4a}$$

$$\frac{d\rho}{dt} = B\left\{\frac{U_a}{\rho} - k(1-s)\right\}, \quad \text{if } U_a/\rho \leq k(1-s), \tag{4b}$$

$$\frac{d\rho}{dt} = 0, \quad \text{if } U_a/\rho > k(1-s) \text{ and } U_a/\rho < k(1+s). \tag{4c}$$

A visualization of equation (4) is given in Figure 1.

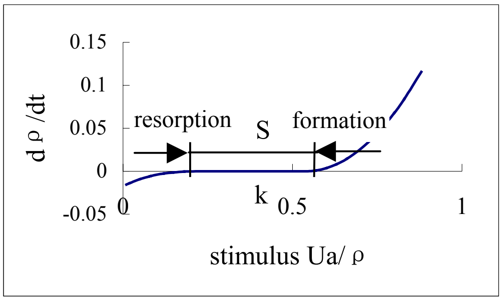

Figure 1. Relationship between density rate and stimulus

When the stimulus value is between k±sk, no bone remodeling will occur. If the stimulus value is outride this range, bone formulation or resorption takes place. According to the actual situation, for an equal value of the driving force U_a/ρ -k, the rate of density changes for resorption is larger than the rate of change in density change for formulation. Thus, Eq.(4) can be expressed as

$$\Delta\rho = B_1\left\{\frac{U_a}{\rho} - k(1 \pm s)\right\}^{\alpha}\Delta t\ , \quad \text{if } U_a/\rho \geq k(1+s) \text{ or } U_a/\rho \leq k(1-s), \tag{5}$$

where subscript α represents 2 or 3 respectively for formation or resorption. The boundary conditions for the predicted apparent densities is expressed as:

$$\rho_{\min} \leq \rho \leq \rho_{\max}\ . \tag{6}$$

In the present calculation, Eq.(6) is taken as $0.001<\rho<1.74\text{g/cm}^3$, where 1.74g/cm^3 is the apparent density of the compact bone. A lower boundary of 0.001 (g/cm^3) instead of zero is taken, because zero density will lead to zero stiffness in the finite element analyses, which will give numerical problems. The relation between the elastic modulus and the bone density is tak`en as

$$E = K\rho^P \tag{7}$$

The value of p can be determined by the homogenization method computation of bone material elastic modulus, which usually ranges from 1 to 3. The constant k is often taken between 2000 and 3000.

2.2 Optimality-criterion algorithm

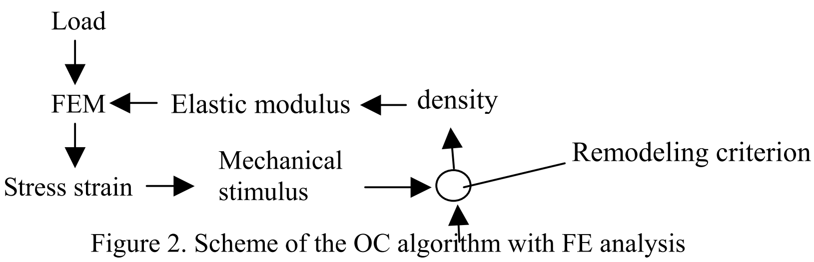

Figure 2. Scheme of the OC algorithm with FE analysis

A schematic representation of the computer simulation process is shown in Figure 2. The main procedures are as follows.

1. The values of stress, strain, and strain-energy density of structural elements of the bone are achieved by the finite element analyses.
2. Based on Eq.(5), we determine whether formation or resorption occurs, which is deduced by strain energy governing equations.
3. For the case of bone remodeling, the density or volume fraction ratio is changed. With the homogenization theory, the elastic modulus of bone can be calculated, and the iteration procedure returns to the finite element analysis of step 1.
4. If the mechanical stimulus does not induce bone remodeling, then the remodeling is finished. When remodeling is finished, it is assumed that the strain-energy density has distributed averagely or most of the bone elements have gotten their limits of the value of density. At that time, the computational process is finished.

The numerical simulation of bone remodeling can be achieved by solving the structural optimization problem via the iteration procedures above described. Based on the remodeling mechanism described in the strain-energy theory, the bone system induces, adjusts, responses, circulates, until the bone material distribution satisfy the optimization criterion of strain energy uniform distribution, which is the normal state of bone. During the computational process, the bone density of every element has its limit. The lower limit is 0, which the bone material is void. The upper limit is 1.74g/cm^3, which is the same as the density of a compact bone.

3 Computational Models

Three models have been adopted to simulate bone remodeling: (1) two-dimensional model of a proximal femur, (2) three dimensional model of a proximal femur. The bone material is assumed to be isotropic. The elastic modulus is 1.43E10Pa/mm^2 and Possion's ratio is 0.43 (Zhu XY, 1997). Multiple load cases are considered in the proximal femur model as shown in Figure 3.

We consider the body weight to be about 800 N. The primary loading case is assumed to result from the stance phase of gait with distributed loads on the femur head and at the attachment of the hip abductor muscles, which is similar in magnitude to those calculated for a single-legged stance. Two distributed loads on the femoral head representing loading from other activities are also incorporated into the model, which are assumed to be 2.4 times the body at the angle of 11^o from the vertical and 0.7 times the body at the angle of 30^o from the vertical respectively. The force due to the pull in the hip abductor muscles is computed as 1263N and inclined at 17^o to the vertical. The force induced by the tibia muscles is 321N and at the angle of 60^o from the vertical.

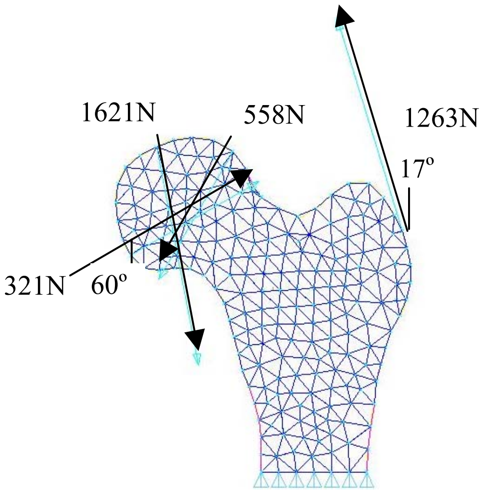

Figure 3. FE model of a proximal femur with loads and boundary conditions

3.1 Two-dimensional models of proximal femur

The 4-node plane membrane element is adopted for the two-dimensional model of the proximal femur. The following four finite element meshes with different numbers of elements are established: (a) 681 nodes and 626 elements; (b) 1109 nodes and 1038 elements; (c) 1889 nodes and 1894 elements; (d) 3087 nodes and 2962 elements.

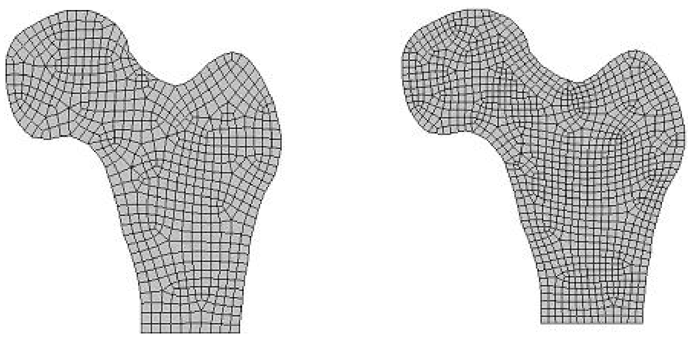

(a) 626 elements (b) 1038 elements

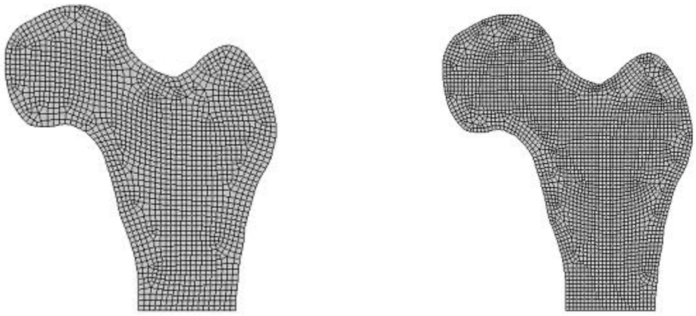

(c) 1894 elements (d) 2962 elements

Figure 4. Finite element meshes of two-dimensional femur

3.2 Three-dimensional models of proximal femur

Three-dimensional model of a proximal femur is formed through processing figure modeling towards computer tomography (CT). As for every piece of CT, the bone figure boundary is picked up and the three-dimensional entity can be produced using the method of surface re-conformation. Thus, the three-dimensional FE model is generated.

The study objective in this paper is the proximal femur of an adult, which is 40 years old and has 175 centimeter of height. The length of the entire bone is about 460 millimeters. 1mm is the basic unit for CT images and 460 images of CT can be obtained. The CT section of each layer is shown in Figure 5. Selecting the part of the entire femur (about 146mm) and processing surface re-conformation, (Figure 6(a)), we can get the entire model, which is shown in Figure 6(b). Figure 6(c) presents the model of the FE mesh with 29192 tetrahedral elements.

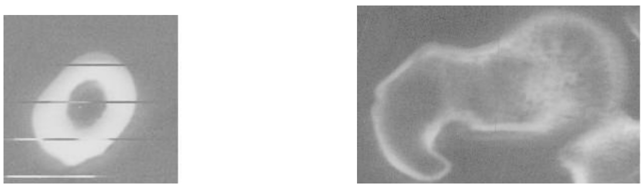

Figure 5. CT image of the cross-section

(a) Outline of a proximal femur with 146 cross-section allayers (b) Solid model of a proximal femur (c) FE model of the femur

Figure 6. Three-dimensional models of a proximal femur

4 Computational Results and Discussions

In the following, based on the strain-energy optimization criterion, simulation results of two and three-dimensional proximal bone models are discussed. Especially the two-dimensional model of the proximal bone is discussed considering the problem of dead zone. The bone fracture healing process is predicted quantitatively, which can provide the mechanism of bone fracture healing.

4.1 Computational analyses

The accuracy of computational results is discussed from the models of the proximal bone with different elemental number, 626 elements and 2940 elements. The uniform strain energy criterion predicts an apparent density distribution, which resembled that of the proximal femur. The results of two-dimensional finite element model of 626 meshes and 2940 meshes are shown in Figure 11(a)(b) and (c) (without of mesh), respectively. The black region denotes the maximal density and the white region denotes the minimal density. Figure 11(d) and (e) are respectively computational results in reference (Charles H.T. et al 1997).

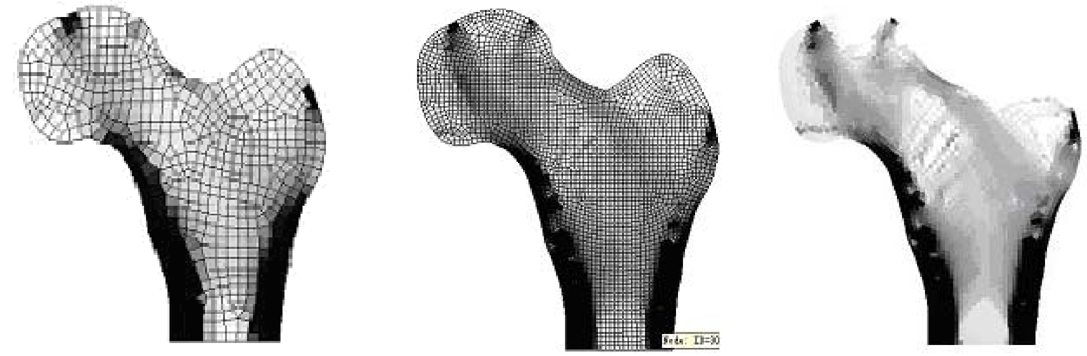

(a) FE model with 626 elements (b) FE model with 2940 elements (c) FE model with 2940 elements

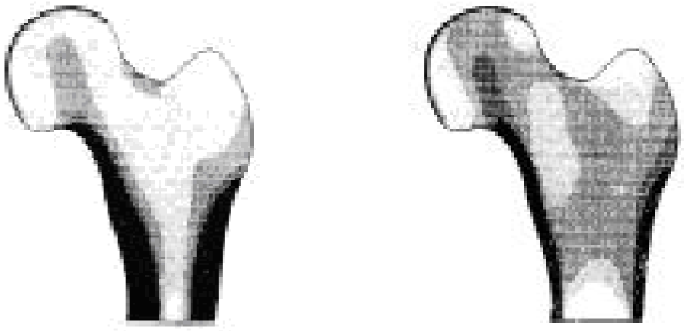

(d) Numerical results in the literature [Christopher et al, 1997] (e) Experiment results in the literature [Christopher et al, 1997]

Figure 11. Results of numerical simulations and experiments

Compared with the results in experiments and literature, it can be concluded that the optimization model of the strain-energy criterion has simulated the bone remodeling process well. The results provide us actual density distribution of the proximal bone. Wolff's law is also verified, i.e. trabecular of cancellous bones grow along the directions of principal stresses. The density distribution of the proximal bone resembles the true density distribution of bone, including the parts of epiphysis and diaphysis of bone. After bone remodeling, the mass loss of epiphysis and diaphysis is given in table 1.

Table 1 Mass loss of bone

Epiphysis parts	Diaphysis parts	Middle part of diaphysis
53.7%	35.2%	24%

The calculated results are in accordance with the actual situation. The bone loss is about 22% to 38% in medicinal experiments. The numerical simulation can explain this phenomenon. The results of the three-dimensional FE model are shown in Figure 12(a). Figure 12(b) provides the result of experiments. The numerical results show that a strain criterion can predict realistically the density distribution.

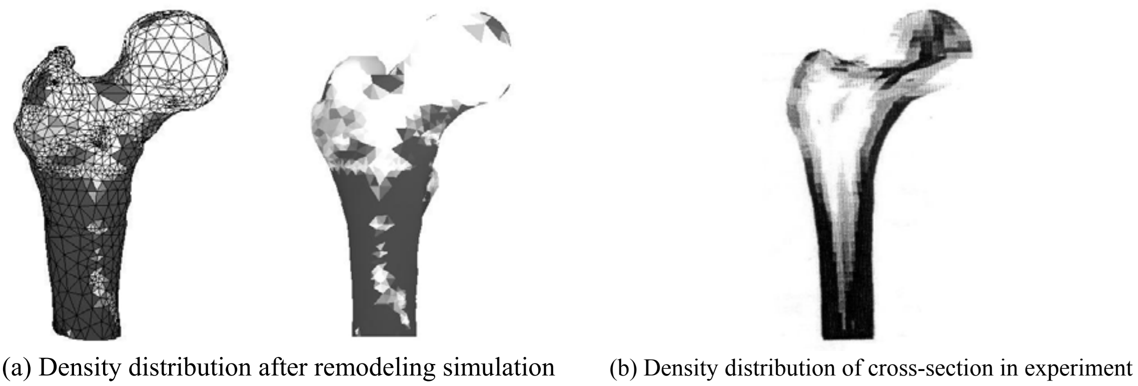

(a) Density distribution after remodeling simulation (b) Density distribution of cross-section in experiment

Figure 12. Numerical simulation results of a three-dimensional proximal femur

4.2 Effect of initial state on bone remodeling

Here we consider two kinds of different initial state. The first one is that the initial model has different apparent density distribution tendency. The second is that the apparent density distribution tendency is the same, but the initial density value is different. In the following we will give the optimization results of these two kinds.

4.2.1 Initial state with different apparent density distribution

To test remodeling algorithms, three different apparent density distributions were used as initial models, which is shown in Figure 13(a)(b)(c). (a) The initial model had a uniform apparent density distribution. (b) The initial model had focal density concentrations. (c) The initial model had a semi-random distribution. The results are shown respectively in Figure 14(a)(b)(c).

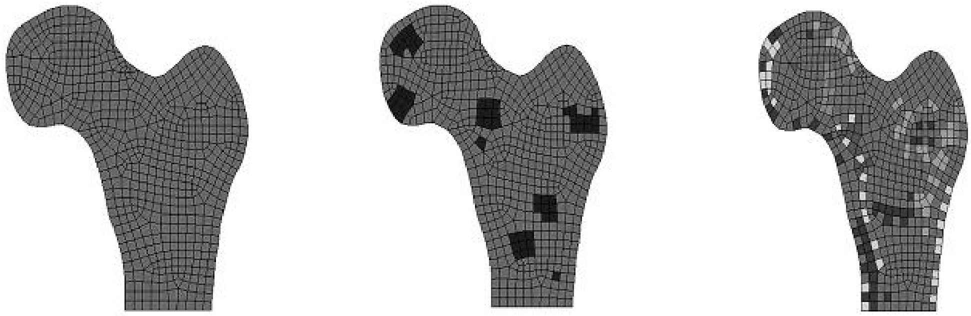

(a) Uniform initial density (b) Local density concentration (c) A semi-random distribution

Figure 13. Initial density distribution

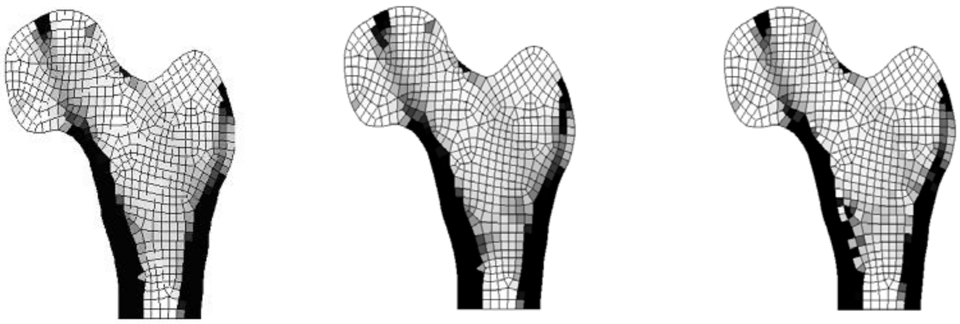

(a) A uniform apparent density distribution (b) Focal density concentrations (c) A semi-random distribution

Figure 14 Density distribution results after bony remodeling

The numerical simulation shows that the results tend to be the same final state in the three cases. That is to say that the bone remodeling has no relation with the initial state. It can also be deduced that the proper loading manner and motion manner can be helpful to recover the fracture bone soon because bone remodeling has almost no relation with the initial state, although the initial state of bone is different so obvious between the normal bone and fracture bone.

4.2.2 Initial state with different apparent density value

The remodeling effects are considered if bone has different initial density values. The five different initial cases of density value are shown in Figure 15(a)-(e). The associated material volume fraction ratios (VFR) are 0.1, 0.3, 0.5, 0.7 and 0.9, respectively. Figure 15(f) is the result of remodeling of all above five cases. It can be concluded that bone remodeling gives the same results although the initial density is different. The total mass ratio with different initial density and different remodeling time is given in Table 2.

(a) μ=0.1 (b) μ=0.3 (c) μ=0.5

(d) μ=0.7 (e) μ=0.9 (f) Remodeling result

Figure 15. Material density distribution under different initial condition

Table 2. Total mass ratio with different initial density and remodeling time

Remodeling time \ VFR	0.1	0.3	0.5	0.7	0.9
10	12.1%	32%	47%	63.1%	80.1%
20	15.3%	35.2%	43.6%	58.0%	73.9%
30	20.5%	40.1%	40.1%	50.1%	54.1%
40	28.1%	38.0%	37.7%	43%	45.9
50	35.5%	35.3%	35%	36%	36.2%

The results show: for the different initial density value, if the time of remodeling is too short, the remodeling results show great differences. With increasing remodeling time, the remodeling results tend to be more closer, until the same density distribution is reached. All above results show that the initial value of density has almost no effect on the remodeling.

4.3 Effect of the dead zone

Dead zone, called lazy zone, is the region of no formation or resorption. Figure 1 and Eq.(4) have explained the phenomenon. If the loading stimulus Ua/ρ does only deviate slightly from the strain-energy density of the normal equilibrium state, no bone remodeling will happen. When the stimulus does significantly exceed the strain-energy density of the normal equilibrium state, bone formation will take place. On the other hand, if the stimulus is significantly lower than the strain-energy density of the normal equilibrium state, bone resorption will occur. The scope of dead zone is not determined, which can be large or small. Usually the value of s is between 0 and 1. When s>0.35, the bone remodeling will become slow and most of the bone elements are almost in their dead state, which is not true. So the value of s is selected between 0 and 0.35. Hence, 12 cases of different dead zones are simulated. The value of s ranges from 0.1 to 0.6 and the step is 0.05. The remodeling numerical simulation results are shown in Figure 16(a)-(c), where s is 0.1, 0.35 and 0.6, respectively.

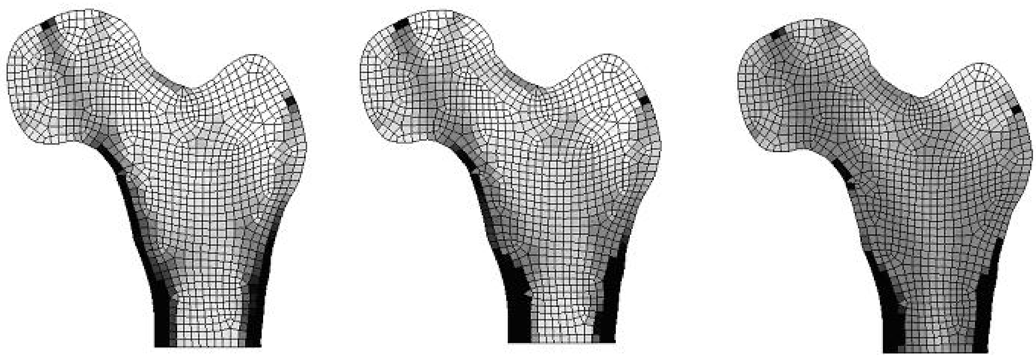

(a) s=0.1 (b) s=0.35 (c) s=0.6

Figure 16. Bone density distribution with different dead zone magnitudes

Table 3. Relationship between dead zone magnitude and midst element number

s	0.1	0.15	0.2	0.25	0.3	0.35	0.4	0.46	0.5	0.55	0.6
Element number	103	171	190	235	389	456	567	613	681	746	896

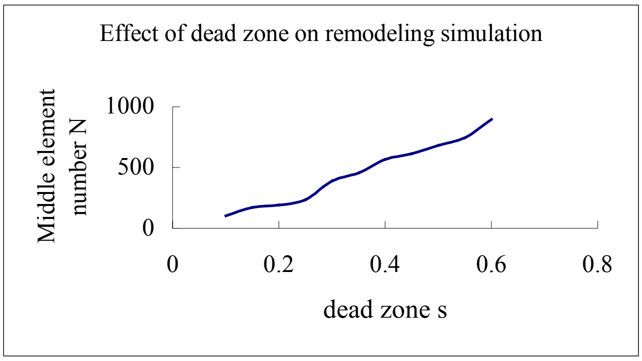

Figure 17. Effect of dead zone on remodeling simulation

The results in Figure 16 are obtained after 40 iterations thereby the initial and loading conditions are the same. It indicates that: 1) the magnitude of s show high effect on the bone remodeling. If s is equal to 0.1, the element number of 1 density or 0 density becomes more. With increasing s, the element number of middle density adds. When s reaches 0.6, most of bone elements are in an inert state, where no bone formation or resorption occur. 2) It can be deduced that the age has some relations with s. Table 3 and Figure 17 may explain the relation between s and the middle element number again. Here the middle element is that whose volume fraction ratio is between 0.35 and 0.7.

4.4 Effect of reference strain energy density

The value of k in Eq.(3) is the reference strain energy density of physiological equilibrium state, which can reflect the normal physiological state. The value of k has high effect on the bone remodeling. The reference strain energy density is different in different physiological phases and regions of bone. In the following, the effect of the magnitude of b on the bone remodeling is illustrated.

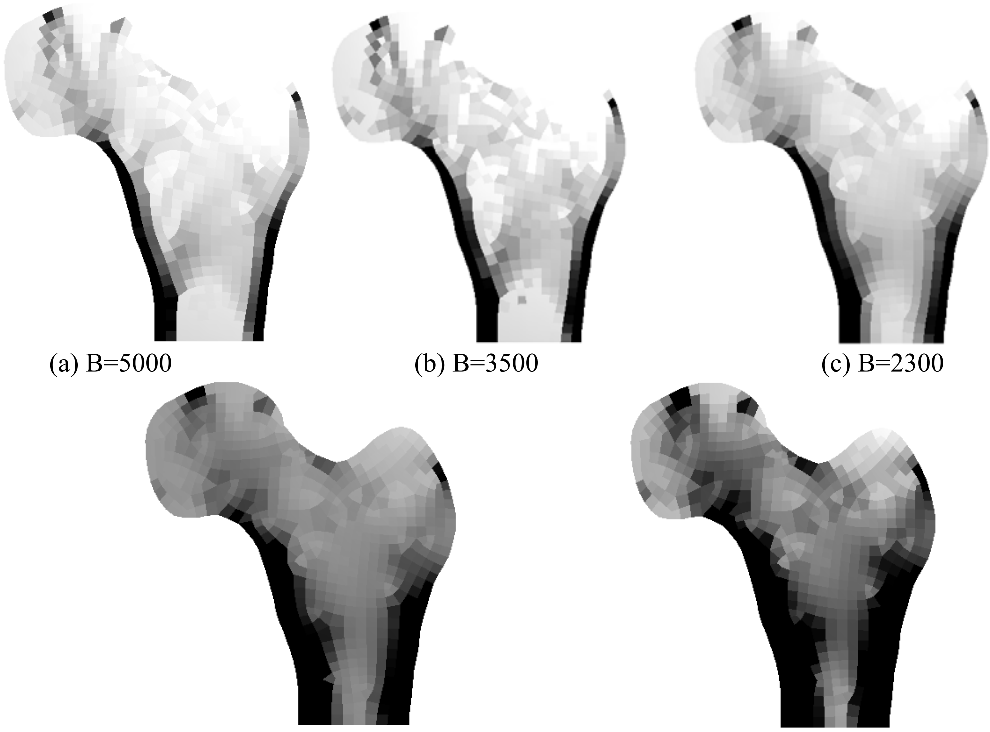

(a) B=5000 (b) B=3500 (c) B=2300

(d) B=1000 (e) B=300

Figure 18. Effect of different reference strain value on remodeling simulation

The remodeling results of different reference strain-energy-densities are shown in Figure 18. From Fig. 18 we conclude: if the value of B changes, the results of bone remodeling will also change. With decreasing B decreasing, the internal material of the bone will become denser, i.e. the element number of 0 density will become less and less and the element number of 1 density will become more and more. When the value of B is very small, the proportion of compact bone in the femur will be considerable large. Considering the actual situation of bone remodeling, we choose the value of B between 2000 and 3000.

4.5 Time dependency of bone remodeling

The bone remodeling coefficient represents the speed of remodeling. When the bone remodeling ratio coefficient is increasing, the bone formation and resorption will become faster. The remodeling ratio coefficient is related to the material properties of bone. The remodeling ratio is different in the different organism even only in the different region of the identical organism. The remodeling ratio coefficient depends on the bone information of gene, which is the result of natural selection. But the selection depends on the mechanical environment. So it is to say that the mechanical environment will alter remodeling ratio coefficient to some degrees. For example, the proper exercise manners after operation will be helpful in shorting recover time.
The bone remodeling ratio coefficient also depends on the age. In the process of growth, the remodeling ratio coefficient is also changing. The bone remodeling ratio coefficient is larger if one is young. With age increases, the metabolism is stable and the remodeling ratio coefficient turns less. When age increases to some degrees, the remodeling ratio coefficient increases and some bone material degenerates little by little.
In Eqs.(3) and (4), B_1 is the remodeling ratio coefficient relative to time. In the course of bone remodeling, based on the changing of bone remodeling ratio coefficient, Eq.(8) is constructed to illuminate the time dependency of bone remodeling.

$$B = p + qe^{-Rt} . \qquad (8)$$

The value B is changing between 200 and 2000. When t denotes 0, the value of B is 2000. With the time passing, the value of B decreases gradually. Eq.(8) can be replaced by

$$B = 200 + 1800e^{-0.0065t} . \qquad (9)$$

Figure 19 represents the time dependency of bone remodeling. The remodeling results with different B are shown in Figure 20. The value of B is selected as 200, 500, 800 and 2000. The results show that remodeling differs obviously after 25 iterations, if the bone remodeling ratio coefficient changes between 200 and 2000. For the case that the value of B becomes larger, formation and resorption will be faster.

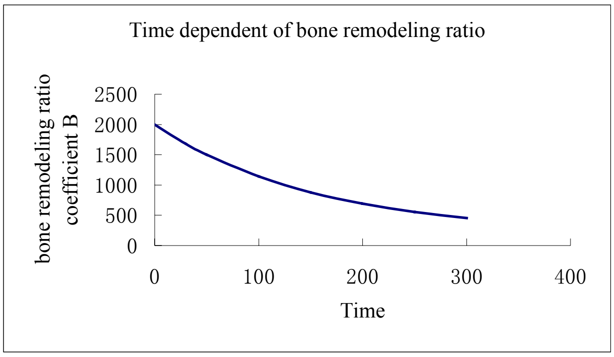

Figure 19. Time dependent of bone remodeling ratio

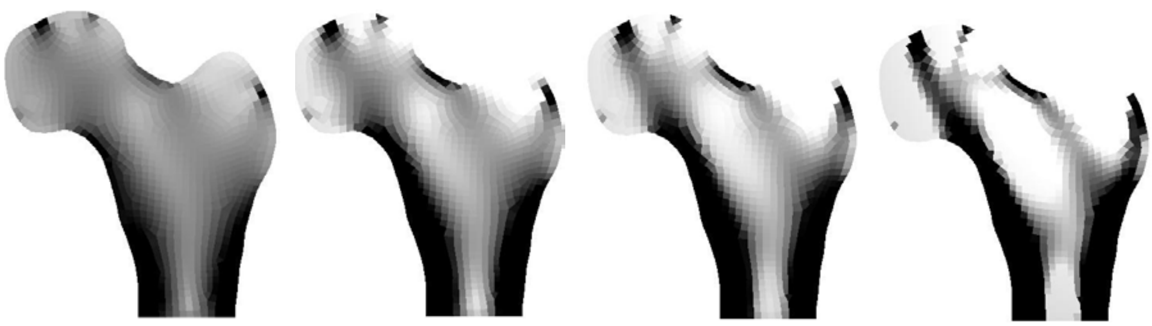

(a) B_2=200 (b) B_2=500 (c) B_2=800 (d) B_2=2000

Figure 20. Bone material distribution with different remodeling ratio coefficients

5 Conclusions

In this paper, the strain-energy density criterion is applied to construct an optimization algorithm to simulate the internal remodeling of trabecular bones. The finite element method performs the numerical analysis of stress and strain of bones. From the results of remodeling simulation for three typical models, we draw the following conclusions.

1) The results of numerical simulation is accordance with Wolff's law, i.e. the mechanical loading is the main factor driving bone remodeling, and the trabecular align with the directions of principal stress.
2) The internal remodeling of bone is numerically simulated in an accurate manner, and the procedure and effects of dead zone, reference strain energy, and remodeling rate related to age can also be simulated in a satisfying way.
3) The strain-energy density criterion accords with the actual bone remodeling process, which can reflect the characteristics of adaptive remodeling theory.

References

Fung Y.C. Biomechanics, The basic equication of biomechanics. University of California, San Diego, USA. 1990.

Fung Y.C. Biomechanics, Motion, Flow, Stress, and Growth. University of California, San Diego, USA. 1990.

Wloff J. Das Gesetz der. Transformation. der Knochen, Hirschwald, Berlin, 1892; 110-157.

Cowin S.C., Hegedus D.M. Bone remodeling: A theory of adaptive elasticity. J Elasticity, 1976; 6; 313-337.

Firoozbkhsh K, Cowin S.C. An analytical model of pauwels function adaptation mechanism for bone. ASME, J Biomech. Engin., 1981; 103; 246.

Currey J.D. The mechanical adaptations of bones. Princeton Univ. Press, 1984.

Fyhrie D.P., Carter D.R. A unifying principle relating stress to trabecular bone morphology. J. Biomech. 1986, 23, 1-10.

Fyhrie D.P., Schaffler M.B. The adaption of bone apparent density to applied load. J. Biomech. 1995, 28, 135-146.

Charles H.T., Vital A., Ramana M.V. A uniform strain criterion for trabecular bone adaption: do continuum-level strain gradients drive adaptation? J. Biomech. 1997, 30(6), 555-563.

Christopher R.J., Simo J.C., Beaupre G.S. Adaptive bone remodeling incorporating simultaneous density and anisotropy considerations. J. Biomech. 1997, 30(6), 603-613.

Carter D.R. Mechanical loading histories and skeletal biology, J. Biomech. 1987, 20, 785-794.

Stilpner M.A. Various continuum bone remodeling algorithms applied to the proximal femur in two and three dimensions, M. Sc. Thesis, Department of Mechanical Engineering, University of Cape Town

Huiskes R., Weinans H., Van Rietbergen B. The relationship between stress shielding and bone resorption around total hip stems and the effects of flexible materials. Clinical Orth. and Related Research, 1992, 274, 124-134.

Poss R., Robertson D., Walker P.S. and et al. Non-cemented total hip arthroplasty. Chap. 30: anatomic stem design for press-fit and cemented application, ed. R. Fitzgerald Jr. Raven Press, New York, 1988.

Angelo C., Marco V. and et al. Global asymptotic stability of bone remodeling theories: a new approach based on non-linear dynamical systems analysis. J. Biomechanics. 1998, 31, 289-294.

Martin L., Overgaard S. and et al. Transforming growth factor-β1 adsorbed to tricalciumphosphate coated impants increases peri-implant bone remodeling. Biomaterial, 2001, 22, 189-193.

Treharne R.W. Review of Wolff's law and its proposed means of operation. Orthop Rev, 1981, 10, 35-47.

Weinbaum S, Cowin S.C., Zeng Y. A model for the excitation of osteocytes by mechanical loading-induced bone fluid shear stress. J. Biomechanics, 1994, 27, 339-360.

Zhu X.Y., Bai F.D., Dong X. and et al. Fumur face remodeling simulation after internal fixation with trihedral fix trough compression plate, Chinese Journal of Biomedical Engineering, 1997, 16(2), 128-133.

Zhang C.Q., Zhu X.Y., Mechanics in plastic stage of fracture union. Chinese Journal of Biomedical Engineering, 2002, 21(2), 132-137.